Electronic Supplementary Material (ESI) for Nanoscale Advances.

Supporting Information

A simple and straightforward strategy for synthesis of N,P co-doped porous carbon: An efficient support of Rh nanoparticles for dehydrogenation of ammonia borane and catalytic application

Wenxiu Luo, Xue Zhao, Wei Cheng, Yun Zhang, Yi Wang*, Guangyin Fan*

The Department of Chemical Engineering and Materials, Sichuan Normal University, Chengdu, China

* Corresponding author: wangyi@sicnu.edu.cn; fanguangyin@sicnu.edu.cn

Table of Contents

Experimental details

Materials

$RhCl_3 \cdot nH_2O$ (Rh content of 39 wt%) was purchased from Precious Metals Institute of Kunming, China. Adenosine triphosphate disodium ($C_{10}H_{14}N_5Na_2O_{13}P_3$, ATP-$Na_2$) was provided by Aladdin Reagent Company of Shanghai, China. Ammonia broane (AB, 90 %) was purchased from Sigma-Aldrich. All chemicals were used without any purification. Deionized water was used in all experiments.

Preparation of porous carbon (ATP-C) derived from adenosine triphosphate disodium (ATP)

In a typical process, adenosine triphosphate disodium (3.0 g) was evenly putted into two porcelain boats, which was subsequently placed in a quartz tube and heated at 800 ℃ for 2 hours (at a slow heating rate of 5 ℃/min) under Ar atmosphere (flow rate of 30 mL/min). After that, a gray-black solid was obtained and then grounded into a powder in an agate mortar. After washed with 1.0 M HCl and deionized water until the washing effluent reached neutral with a pH of 7 at room temperature, the powder was dried at 100 ℃for 12 h. The obtained carbon was named as ATP-C-800. To further investigate the temperature effect of pyrolysis, the carbonization temperatures of the porous carbons through the similar treatment were 700 ℃ and 900 ℃, respectively. The final porous carbons were denoted as ATP-C-700, ATP-C-900, indicating the different carbonization temperature.

Preparation of Rh(III)/ATP-C

In a typical synthesis, 50 mg of ATP-C was stirred in 20 mL methanol and dispersed for 20 min. After that, 7.4 mg $RhCl_3 \cdot nH_2O$ was added into the solution and the mixture was continually stirred in water bath at constant temperature of 60 ± 0.2 ℃. The solution was evaporated and the black powder of Rh(III)/ATP-C with 5.8 wt % Rh loading was obtained finally. Furthermore, the corresponding of Rh(III)/ATP-C with 5 wt % Rh loading and 6.5 wt % Rh loading were synthesized to measure the trend of hydrolytic performance.

In situ formation of Rh/ATP-C and catalytic hydrolysis of AB by Rh/ATP-C

Specifically, 10 mg of Rh(III)/ATP-C was dispersed in 4 mL deionized water kept in a 25 mL two-neck flask. One neck of the flask was connected to a gas burette to measure the volume of hydrogen. After ultrasonicating for 20 min, the mixture was putted in a magnetic stirrer keeping constant temperature at 25 ± 0.2 ℃. A solution of BH_3NH_3 in 1.0 mL deionized water solution (containing 1.0 mmol of AB) was quickly injected into the reactor by a syringe. The catalytic hydrolysis of AB started immediately and Rh nanoparticles were supported on ATP-C, and the Rh/ATP-C catalyst was formed. For catalytic hydrolysis of AB by Rh/ATP-C catalyst, after the first run of hydrogen generation reaction was completed, the Rh/ATP-C catalyst was isolated from the reaction mixture and rinsed by water. The recovered black solid was transferred into the reactor and another 1.0 mole of AB aqueous solution was subsequently added to the reaction system. The released gas monitored by the gas burette and the reaction was completed when there was no more gas generation.

The TOF for hydrolytic decomposition of AB was calculated based on the number of Rh atoms in catalysts according to the following Equation S1:

$$\mathrm{TOF} = \frac{P_{atm}V_{H_2}/RT}{n_{Rh}t} \qquad (\mathrm{S1})$$

where P_{atm} is the atmospheric pressure (101325 Pa), V_{H2} is the volume of H_2 generated at the time (t) of half-completion of H_2 generation, R is the universal gas constant (8.3145 m^3 Pa mol^{-1} K^{-1}), T is reaction temperature (298 K), n_{Rh} is the total mole number of Rh atoms in catalyst.

The reusability of the Rh/ATP-C catalyst was determined using the recovered catalyst after hydrolytic decomposition of AB. The recovered Rh catalyst from each cycle was washed three times with water and ethanol. When the fresh AB aqueous solution was introduced, the next recycling run was started. Recycling tests were repeated for eight times.

UV-vis Absorption Spectrum Measurements of 4-nitrophenol

The UV-vis absorption spectra of 4-nitrophenol (4-NP) in the presence of NH_3BH_3 were monitored over the wavelength range from 250 to 500 nm. The process was carried out in a wellstoppered quartz cuvette. In a typical process, 0.2 mL of the Rh/ATP-C catalysts dispersion (0.2 mg/mL) was added to 2 mL of 4-NP stock solution (0.0625 mM). Then 1 mL of freshly prepared NH_3BH_3 aqueous solution (contain 1 mmol NH_3BH_3) was added to the above solution and UV-visible absorption spectra were monitored at different time intervals.

Characterization

Powder X-ray diffraction (XRD) measurements were carried out using a Rigaku Ultima IV diffractometer with Cu Kα radiation. Scanning electron microscopy (SEM) images were taken using a JEOL JSM-5310LVat 15 kV and 33 Pa in a low-vacuum mode without metal coating on aluminum support. The morphologies of all the samples were observed using a transmission electron microscope (TEM, JEM-2010) equipped. The *X*-ray photoelectron spectra (XPS) were acquired with an ESCALAB250 (Thermo VG Corp). FT-IR spectra were collected at room temperature by using a Thermo FTIR-iS10 instrument using KBr discs in the 400−4000 cm^{-1} region. Surface area of the samples is calculated by the Brunauer-Emmet-Teller (BET) method.

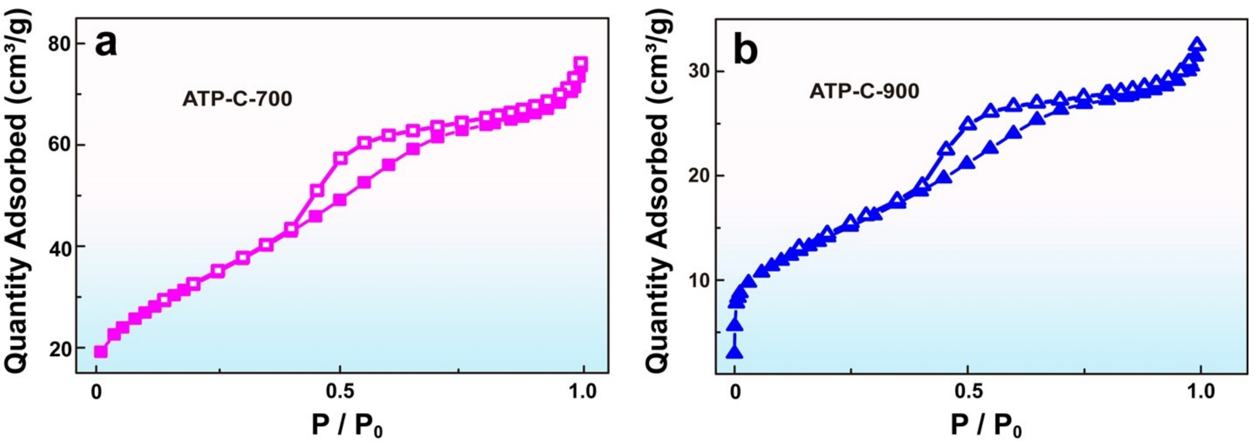

Figure S1. The BET spectra of (a) ATP-C-700 and (b) Rh/ATP-C-900.

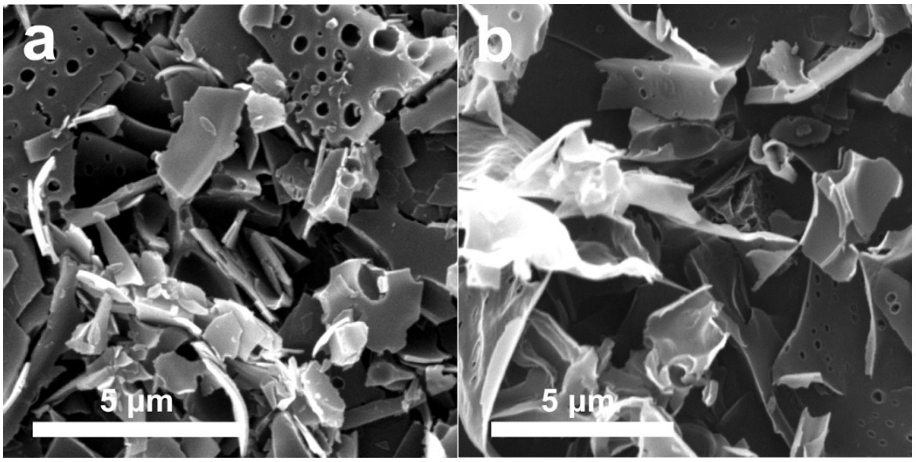

Figure S2. The SEM spectra of (a) ATP-C-700 and (b) Rh/ATP-C-900

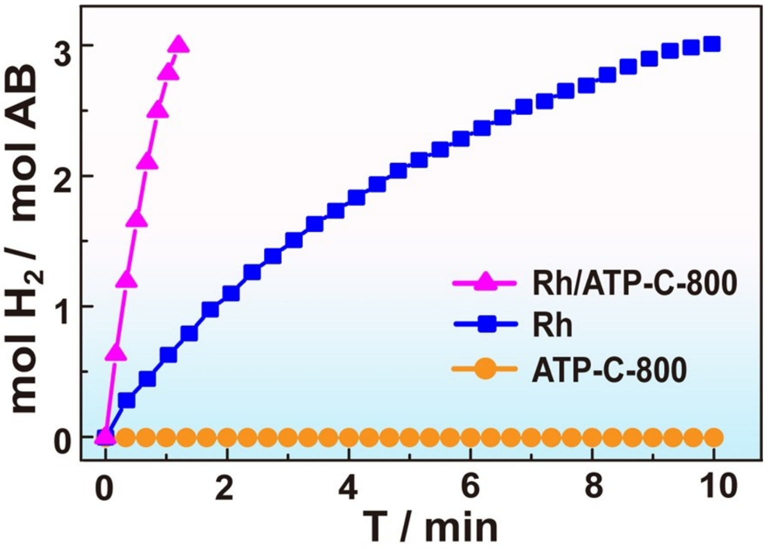

Figure S3. H_2 generation rate of AB hydrolysis catalyzed by Rh/ATP-C-800, Rh, ATP-C-800, respectively.

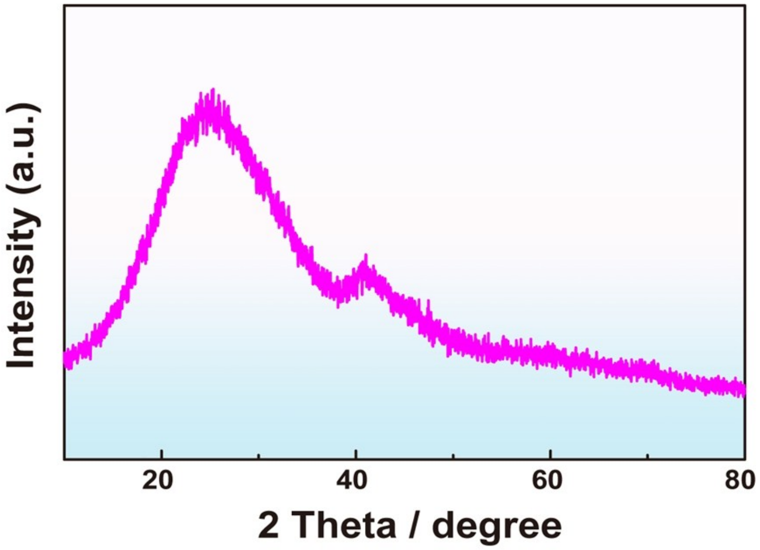

Figure S4. The XRD patterns of Rh/ATP-C-800 after eight runs of recycling for hydrolytic decomposition of AB

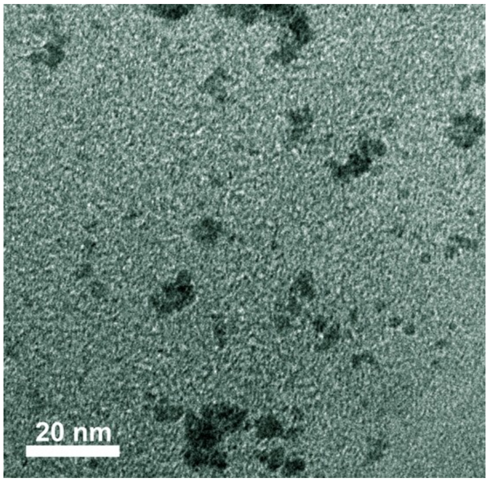

Figure S5. TEM patterns of Rh/ATP-C-800 after eight runs of recycling for hydrolytic decomposition of AB

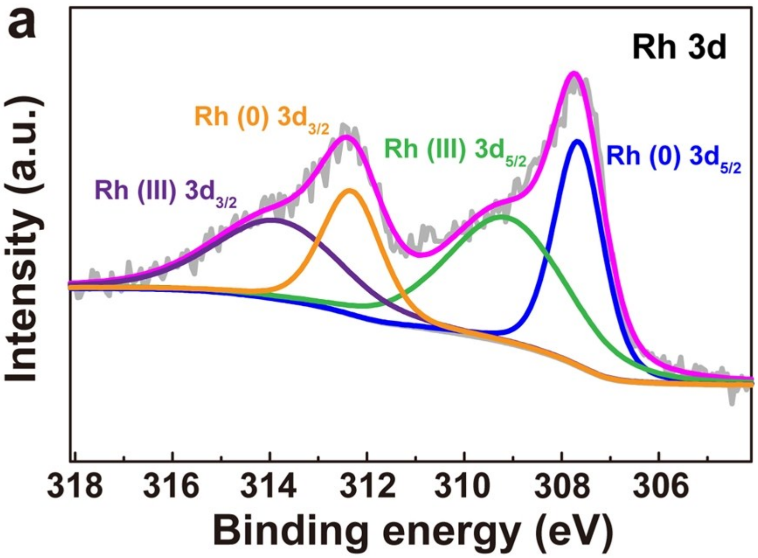

Figure S6. The XPS spectrum of Rh3d in ATP-C-800 after eight runs of recycling for hydrolytic decomposition of AB, respectively.

Table S1. Comparison of catalytic activity of reported Rh-based catalysts for AB hydrolysis.

Catalysts	**TOF(min)$^{-1}$**	**E_a (kJ/mol)**	**References**
Rh/CeO_2	2010	42.6	1
in situ-Rh/C	1246	40.9	2
Rh/g-C_3N_4	969	24.2	3
Rh/CNT	706	32	4
Rh^0 /nanoTiO_2	643	47	5
Rh/Carbon-SC	336	37.1	6
Rh/graphene	325	19.7	7
Rh/P(triaz)	260	-	8
RhNPs/1[a]	244	26.1	9
Rh-3D-2D[b]	136.4	19.9	10

[a] ‘1’refer to water-soluble arene-centered triethylene glycol (TEG)-terminated “click” dendrimers.

[b] Rh-3D-2D refer to ultrathin Rh nanosheet nanoassemblies with dendritic morphology.

References

1. Akbayrak, S.; Tonbul, Y.; Özkar, S., Ceria supported rhodium nanoparticles: Superb catalytic activity in hydrogen generation from the hydrolysis of ammonia borane. *Appl. Catal., B* **2016,** *198*, 162-170.

2. Hu, M.; Ming, M.; Xu, C.; Wang, Y.; Zhang, Y.; Gao, D.; Bi, J.; Fan, G., Towards High-Efficiency Hydrogen Production through in situ Formation of Well-Dispersed Rhodium Nanoclusters. *ChemSusChem* **2018**.

3. Lu, R.; Hu, M.; Xu, C.; Wang, Y.; Zhang, Y.; Xu, B.; Gao, D.; Bi, J.; Fan, G., Hydrogen evolution from hydrolysis of ammonia borane catalyzed by Rh/g-C3N4 under mild conditions. *Int. J. Hydrogen Energy* **2018,** *43* (14), 7038-7045.

4. Yao, Q.; Lu, Z.-H.; Jia, Y.; Chen, X.; Liu, X., In situ facile synthesis of Rh nanoparticles supported on carbon nanotubes as highly active catalysts for H2 generation from NH3BH3 hydrolysis. *Int. J. Hydrogen Energy* **2015,** *40* (5), 2207-2215.

5. Tonbul, Y.; Akbayrak, S.; Özkar, S., Group 4 oxides supported Rhodium(0) catalysts in hydrolytic dehydrogenation of ammonia borane. *Int. J. Hydrogen Energy* **2019,** *44* (27), 14164-14174.

6. Chen, J.; Hu, M.; Ming, M.; Xu, C.; Wang, Y.; Zhang, Y.; Wu, J.; Gao, D.; Bi, J.; Fan, G., Carbon-supported small Rh nanoparticles prepared with sodium citrate: Toward high catalytic activity for hydrogen evolution from ammonia borane hydrolysis. *Int. J. Hydrogen Energy* **2018,** *43* (5), 2718-2725.

7. Shen, J.; Yang, L.; Hu, K.; Luo, W.; Cheng, G., Rh nanoparticles supported on graphene as efficient catalyst for hydrolytic dehydrogenation of amine boranes for chemical hydrogen storage. *Int. J. Hydrogen Energy* **2015,** *40* (2), 1062-1070.

8. Sun, J.-K.; Kochovski, Z.; Zhang, W.-Y.; Kirmse, H.; Lu, Y.; Antonietti, M.; Yuan, J., General Synthetic Route toward Highly Dispersed Metal Clusters Enabled by Poly(ionic liquid)s. *J. Am. Chem. Soc.* **2017,** *139* (26), 8971-8976.

9. Wang, Q.; Fu, F.; Escobar, A.; Moya, S.; Ruiz, J.; Astruc, D., “Click” Dendrimer-Stabilized Nanocatalysts for Efficient Hydrogen Release upon Ammonia-Borane Hydrolysis. *ChemCatChem* **2018,** *10* (12), 2673-2680.

10. Bai, J.; Xu, G.-R.; Xing, S.-H.; Zeng, J.-H.; Jiang, J.-X.; Chen, Y., Hydrothermal Synthesis and Catalytic Application of Ultrathin Rhodium Nanosheet Nanoassemblies. *ACS Appl. Mater. Interfaces* **2016,** *8* (49), 33635-33641.